WATER RESOURCES RESEARCH, VOL. 31, NO. 5, PAGES 1429–1437, MAY 1995

Analytical models for one-dimensional virus transport in saturated porous media

Youn Sim and Constantinos V. Chrysikopoulos
Department of Civil and Environmental Engineering, University of California, Irvine

Abstract. Analytical solutions to two mathematical models for virus transport in one-dimensional homogeneous, saturated porous media are presented, for constant flux as well as constant concentration boundary conditions, accounting for first-order inactivation of suspended and adsorbed (or filtered) viruses with different inactivation constants. Two processes for virus attachment onto the solid matrix are considered. The first process is the nonequilibrium reversible adsorption, which is applicable to viruses behaving as solutes; whereas, the second is the filtration process, which is suitable for viruses behaving as colloids. Since the governing transport equations corresponding to each physical process have identical mathematical forms, only one generalized closed-form analytical solution is developed by Laplace transform techniques. The impact of the model parameters on virus transport is examined. An empirical relation between inactivation rate and subsurface temperature is employed to investigate the effect of temperature on virus transport. It is shown that the differences between the two boundary conditions are minimized at advection-dominated transport conditions.

Introduction

The transport and fate of viruses in porous media are mainly governed by virus attachment onto the solid matrix and inactivation [*Vilker*, 1981]. Interactions between suspended viruses and solid surfaces are often described by physical equilibrium adsorption models such as the Langmuir and Freundlich isotherms. Both isotherms assume that adsorption is an instantaneous process, sorbed and liquid phase virus concentrations are in equilibrium, and the adsorbate is conservative (i.e., nondecaying) [*Morel*, 1983]. Therefore these isotherms may not be applicable to virus sorption, because they cannot account for deviations from equilibrium due to continuous virus inactivation [*Grant et al.*, 1993]. *Vilker* [1981] suggested that the nonequilibrium adsorption process is appropriate for models describing virus transport in porous media. This adsorption process represents the rate of approach to equilibrium between adsorbed and liquid phase virus concentrations, accounting for virus transport to the outer layer of a solid particle by mass transfer followed by virus immobilization. The colloid filtration theory is frequently applied to virus transport in porous media. Colloids are filtered by a solid matrix through interception, sedimentation (mechanical filtration), and diffusion. Since the interception and sedimentation processes are effective only for large-size particles (≥ 1 μm), for the case of virus filtration the effects of sedimentation and interception can be neglected [*Harvey and Garabedian*, 1991].

Inactivation of suspended as well as sorbed or attached viruses is an irreversible sink mechanism that is commonly described by a first-order rate expression [*Yates and Yates*, 1988]. It has been reported that the inactivation rate is smaller for attached than suspended viruses [*Hurst et al.*, 1980; *Gerba*, 1984; *Yates and Yates*, 1988]. Thus inactivation rates of suspended and attached viruses should not be assumed equal. The most important factor for virus inactivation in the subsurface is temperature [*Corapcioglu and Haridas*, 1984]. Viruses remain infective much longer at lower temperatures (1°–8°C) than at higher temperatures (20°–32°C) [*Sobsey*, 1983; *Park et al.*, 1992]. Correlations of virus inactivation rates with temperature have been reported by *Reddy et al.* [1981] and *Yates et al.* [1985].

There are several mathematical models available in the literature for virus transport in porous media. Some of these models treat viruses as solutes due to their small size [*Grosser*, 1984; *Tim and Mostaghimi*, 1991; *Park et al.*, 1992; *Vilker et al.*, 1978]. Other virus transport models have adopted the well-established filtration theory to account for virus deposition onto the solid matrix [*Matthess et al.*, 1988; *Teutsch et al.*, 1991; *Yates and Ouyang*, 1992].

The present work extends the collection of virus transport analytical models. Viruses behaving both as solutes and colloids are examined. The impact of first-order inactivation of suspended as well as adsorbed (or filtered) viruses with different inactivation constants is investigated. The effect of available boundary conditions and subsurface temperature on virus transport is explored. Finally, existing virus breakthrough experimental data are successfully simulated.

Development of Models

The one-dimensional virus transport in homogeneous, saturated porous media with first-order adsorption (or filtration) and inactivation is governed by the following partial differential equation:

$$\frac{\partial C(t,x)}{\partial t} + \frac{\rho}{\theta}\frac{\partial C^*(t,x)}{\partial t} = D\frac{\partial^2 C(t,x)}{\partial x^2} - U\frac{\partial C(t,x)}{\partial x} - \lambda C(t,x) - \lambda^* \frac{\rho}{\theta} C^*(t,x), \quad (1)$$

where C is the concentration of virus in suspension; C^* is the mass of virus adsorbed on the solid matrix; D is the hydrody-

Paper number 95WR00199.
0043-1397/95/95WR-00199$05.00

namic dispersion coefficient; U is the average interstitial velocity; ρ is the bulk density of the solid matrix; λ is the inactivation constant of suspended viruses; λ^* is the inactivation constant of adsorbed viruses; θ is the porosity of soil medium; and t is time. The left-hand side of the preceding equation consists of the accumulation terms, and the last two terms represent the inactivation of suspended and adsorbed viruses, respectively. The rate of virus attachment onto the solid matrix is described by the following generalized expression:

$$\frac{\rho}{\theta}\frac{\partial C^*(t, x)}{\partial t} = r_1 C(t, x) - r_2 C^*(t, x), \tag{2}$$

where r_1 and r_2 are the forward and the reverse rate coefficients.

The desired expression for C^* is obtained by solving (2) subject to an initial condition of zero sorbed (or filtered) virus concentration ($C^*(0, x) = 0$) as

$$C^*(t, x) = \frac{r_1\theta}{\rho}\int_0^t C(\tau, x)\exp\left[-\frac{r_2\theta}{\rho}(t-\tau)\right]d\tau. \tag{3}$$

In view of (2) and (3) the governing equation (1) can be written as

$$\frac{\partial C(t, x)}{\partial t} = D\frac{\partial^2 C(t, x)}{\partial x^2} - U\frac{\partial C(t, x)}{\partial x} - \mathcal{A}C(t, x) - \mathcal{B}\int_0^t C(\tau, x)e^{-\mathcal{H}(t-\tau)}d\tau, \tag{4}$$

where the following substitutions have been employed:

$$\mathcal{A} = r_1 + \lambda, \tag{5}$$

$$\mathcal{B} = r_1(\lambda^* - \mathcal{H}), \tag{6}$$

$$\mathcal{H} = \theta r_2/\rho. \tag{7}$$

For a semi-infinite one-dimensional porous medium in the presence of a continuous source of viruses, the appropriate initial and boundary conditions are

$$C(0, x) = 0, \tag{8}$$

$$-D\frac{\partial C(t, 0)}{\partial x} + UC(t, 0) = UC_0, \tag{9}$$

$$C(t, 0) = C_0, \tag{10}$$

$$\frac{\partial C(t, \infty)}{\partial x} = 0, \tag{11}$$

where C_0 is the source concentration. It should be noted that for a given problem either (9) or (10) is used for constant flux and constant concentration boundary condition cases, respectively, but not both. The condition (8) establishes that there is no initial virus concentration within the one-dimensional porous medium. The constant flux boundary condition (9) implies virus concentration discontinuity at the inlet. Condition (10) represents the constant concentration boundary condition. The downstream boundary condition (11) preserves concentration continuity for a semi-infinite system. For the case of constant flux boundary condition, (4) subject to conditions (8), (9) and (11) is solved analytically following the methods of *Lapidus and Amundson* [1952] and *Chrysikopoulos et al.* [1990]. Taking Laplace transforms of (4), (8), (9), and (10) with respect to time and space yields

$$s\tilde{C}^*(s, \gamma) - C^*(0, \gamma) = D\left[\gamma^2\tilde{C}^*(s, \gamma) - \gamma\tilde{C}(s, 0) - \frac{d\tilde{C}(s, 0)}{dx}\right] - U[\gamma\tilde{C}^*(s, \gamma) - \tilde{C}(s, 0)] - \mathcal{A}\tilde{C}^*(s, \gamma) - \frac{\mathcal{B}}{s+\mathcal{H}}\tilde{C}^*(s, \gamma), \tag{12}$$

$$C^*(0, \gamma) = 0, \tag{13}$$

$$-D\frac{d\tilde{C}(s, 0)}{dx} + U\tilde{C}(s, 0) = \frac{UC_0}{s}, \tag{14}$$

$$\frac{d\tilde{C}(s, \infty)}{dx} = 0, \tag{15}$$

where the tilde and solid degree sign signify Laplace transform with respect to time and space, respectively, and s and γ are the corresponding Laplace domain variables. Substituting boundary conditions (13) and (14) into (12) and solving for $\tilde{C}^*(s, \gamma)$, yields

$$\tilde{C}^*(s, \gamma) = \frac{\gamma\tilde{C}(s, 0) - (UC_0/sD)}{(\gamma + M + N)(\gamma + M - N)}, \tag{16}$$

where the following substitutions have been employed:

$$M = -U/2D, \tag{17a}$$

$$N = \left(\frac{s}{D} + \frac{\mathcal{A}}{D} + \frac{U^2}{4D^2} + \frac{\mathcal{B}}{D(s+\mathcal{H})}\right)^{1/2}. \tag{17b}$$

Using the following Laplace inversion identities [*Roberts and Kaufman*, 1966]

$$\mathcal{L}^{-1}\left\{\frac{\gamma}{(\gamma + M + N)(\gamma + M - N)}\right\} = \frac{(M+N)e^{-(M+N)x} - (M-N)e^{-(M-N)x}}{2N}, \tag{18}$$

$$\mathcal{L}^{-1}\left\{\frac{1}{(\gamma + M + N)(\gamma + M - N)}\right\} = \frac{e^{-(M-N)x} - e^{-(M+N)x}}{2N}, \tag{19}$$

where $\mathcal{L}^{-1}$ is the Laplace inverse operator, the inverse Laplace transform of (16) with respect γ is obtained as

$$\tilde{C}(s, x) = \frac{UC_0}{sD^{1/2}}\exp\left[\frac{Ux}{2D}\right]\left\{\frac{\mathcal{H}}{s+\mathcal{H}}\Theta + \frac{s}{s+\mathcal{H}}\Theta\right\}, \tag{20}$$

where

$$\Theta = \frac{\exp\left[-\frac{x}{D^{1/2}}\left(s + \mathcal{A} + \frac{U^2}{4D} + \frac{\mathcal{B}}{s+\mathcal{H}}\right)^{1/2}\right]}{\frac{U}{2D^{1/2}} + \left(s + \mathcal{A} + \frac{U^2}{4D} + \frac{\mathcal{B}}{s+\mathcal{H}}\right)^{1/2}}. \tag{21}$$

It should be noted that for the evaluation of $\tilde{C}(s, 0)$, which is already substituted in (20), the boundary condition (15) has been employed.

The inverse Laplace transform of (20) with respect to s is obtained by using the following relationship [*Lapidus and Amundson*, 1952]:

$$\mathcal{L}^{-1}\left\{\frac{1}{s+\mathcal{H}}\tilde{f}\left(s+\mathcal{H}+\frac{a}{s+\mathcal{H}}\right)\right\}$$

$$= e^{-\mathcal{H}t}\int_0^t J_0[2(a\zeta(t-\zeta))^{1/2}]f(\zeta)\,d\zeta, \tag{22}$$

where a is a constant, the arbitrary function $f(t)$ is the inverse Laplace transform of $\tilde{f}(s)$, and J_0 is the Bessel function of the first kind of zeroth order. In view of (21), $\tilde{f}(s)$ is assumed to be as follows:

$$\tilde{f}(s) = \frac{\exp\left[-\alpha_1(s+\alpha_2)^{1/2}\right]}{\alpha_3 + (s+\alpha_2)^{1/2}}, \tag{23}$$

where α_1, α_2, and α_3 are constants. Furthermore, in view of the preceding expression

$$\Theta = \tilde{f}\left(s+\mathcal{H}+\frac{a}{s+\mathcal{H}}\right)$$

$$= \frac{\exp\left[-\alpha_1\left(\dfrac{s^2+(2\mathcal{H}+\alpha_2)s+\mathcal{H}^2+\mathcal{H}\alpha_2+a}{s+\mathcal{H}}\right)^{1/2}\right]}{\alpha_3+\left(\dfrac{s^2+(2\mathcal{H}+\alpha_2)s+\mathcal{H}^2+\mathcal{H}\alpha_2+a}{s+\mathcal{H}}\right)^{1/2}}. \tag{24}$$

The inverse Laplace transform of (23) is [*Roberts and Kaufman*, 1966]

$$f(t) = \frac{1}{(\pi t)^{1/2}}\exp\left[\frac{-\alpha_1^2}{4t}-\alpha_2 t\right] - \alpha_3\exp\left[\alpha_1\alpha_3+(\alpha_3^2-\alpha_2)t\right]$$

$$\cdot\operatorname{erfc}\left[\frac{\alpha_1}{2t^{1/2}}+\alpha_3 t^{1/2}\right]. \tag{25}$$

By simple comparison of (21) and (24), the unknown constants are evaluated:

$$a = \mathcal{B} \tag{26a}$$

$$\alpha_1 = x/D^{1/2} \tag{26b}$$

$$\alpha_2 = \mathcal{A} + (U^2/4D) - \mathcal{H} \tag{26c}$$

$$\alpha_3 = U/2D^{1/2}. \tag{26d}$$

Then, the inverse $\mathcal{L}^{-1}\{\Theta/(s+\mathcal{H})\} = \Phi(t)$ can be determined by combining (22)–(26). Therefore

$$\mathcal{L}^{-1}\left\{\frac{1}{s}\left(\frac{\mathcal{H}}{s+\mathcal{H}}\Theta+\frac{s}{s+\mathcal{H}}\Theta\right)\right\} = \int_0^t \mathcal{H}\Phi(\tau)\,d\tau + \Phi(t), \tag{27}$$

where the convolution theorem has been applied. In view of (20) and (27) the desired general solution for the constant flux boundary condition is obtained as

$$C_{cf}(t,x) = \frac{C_0 U}{D^{1/2}}\exp\left[\frac{Ux}{2D}\right]\left\{\int_0^t\int_0^\tau \mathcal{H}e^{-\mathcal{H}\tau}J_0[2(\mathcal{B}\zeta(\tau-\zeta))^{1/2}]\right.$$

$$\cdot\left\{\frac{1}{(\pi\zeta)^{1/2}}\exp\left[\frac{-x^2}{4D\zeta}+\left(\mathcal{H}-\mathcal{A}-\frac{U^2}{4D}\right)\zeta\right]\right.$$

$$\left.-\frac{U}{2D^{1/2}}\exp\left[\frac{Ux}{2D}+(\mathcal{H}-\mathcal{A})\zeta\right]\right.$$

$$\left.\cdot\operatorname{erfc}\left[\frac{x}{2(D\zeta)^{1/2}}+\frac{U}{2}\left(\frac{\zeta}{D}\right)^{1/2}\right]\right\}d\zeta\,d\tau$$

$$+ e^{-\mathcal{H}t}\int_0^t J_0[2(\mathcal{B}\zeta(t-\zeta))^{1/2}]$$

$$\cdot\left\{\frac{1}{(\pi\zeta)^{1/2}}\exp\left[\frac{-x^2}{4D\zeta}+\left(\mathcal{H}-\mathcal{A}-\frac{U^2}{4D}\right)\zeta\right]\right.$$

$$\left.-\frac{U}{2D^{1/2}}\exp\left[\frac{Ux}{2D}+(\mathcal{H}-\mathcal{A})\zeta\right]\right.$$

$$\left.\cdot\operatorname{erfc}\left[\frac{x}{2(D\zeta)^{1/2}}+\frac{U}{2}\left(\frac{\zeta}{D}\right)^{1/2}\right]\right\}d\zeta\Big\}, \tag{28}$$

where the subscript cf indicates the use of the constant flux upstream boundary condition. For the case of constant concentration boundary condition, the governing integrodifferential equation (4) is solved analytically subject to conditions (8), (10), and (11) in a similar fashion to yield

$$C_{cc}(t,x) = C_0\exp\left[\frac{Ux}{2D}\right]$$

$$\cdot\left\{\int_0^t \mathcal{H}\left(e^{-\mathcal{H}\tau}\int_0^\tau \frac{xJ_0[2(\mathcal{B}\zeta(\tau-\zeta))^{1/2}]}{2(D\pi\zeta^3)^{1/2}}\right.\right.$$

$$\left.\left.\cdot\exp\left[\frac{-x^2}{4D\zeta}+\left(\mathcal{H}-\mathcal{A}-\frac{U^2}{4D}\right)\zeta\right]d\zeta\right)d\tau\right.$$

$$+ e^{-\mathcal{H}t}\int_0^t \frac{xJ_0[2(\mathcal{B}\zeta(t-\zeta))^{1/2}]}{2(D\pi\zeta^3)^{1/2}}$$

$$\left.\cdot\exp\left[\frac{-x^2}{4D\zeta}+\left(\mathcal{H}-\mathcal{A}-\frac{U^2}{4D}\right)\zeta\right]d\zeta\right\}, \tag{29}$$

where the subscript cc indicates the use of the constant concentration upstream boundary condition.

For the special case of $\lambda = \lambda^* = 0$ using the following substitutions: $r_1\theta/\rho = k_1$, $r_2\theta/\rho = k_2$, $\rho/\theta = 1/\varepsilon$, $r_1 = k_1/\varepsilon$, and the Bessel function relationship $I_0(z) = J_0(iz)$, where I_0 is the modified Bessel function of the first kind of zeroth order and z is an arbitrary argument [*Abramowitz and Stegun*, 1972], the analytical solution for the constant concentration boundary condition (29) reduces to the solution presented by *Lapidus and Amundson* [1952]. It should be noted that in the notation of *Lapidus and Amundson* [1952], k_1 and k_2 are the forward and reverse reaction rates, respectively, and ε is the fractional void volume.

Nonequilibrium Adsorption Model (S Model)

Assuming that the adsorption process consists of virus diffusion to the outer layer of a solid particle by nonequilibrium mass transfer, and virus immobilization onto the solid particle while in equilibrium with the liquid phase virus concentration in the outer layer, the sorption term in the governing equation (1) can be written as

$$\frac{\rho}{\theta}\frac{\partial C^*(t,x)}{\partial t} = k[C(t,x) - C_g(t,x)], \qquad (30)$$

where k is the mass transfer rate constant; C_g is the liquid phase virus concentration in direct contact with solids, which is evaluated from an appropriate isotherm relationship. *Vilker* [1981] suggested the Langmuir isotherm

$$C^* = Q^\circ b C_g/(1 + bC_g), \qquad (31)$$

where Q° is the Langmuir monolayer capacity, an ultimate solid phase concentration of adsorbed viruses, and b is a constant related to the bonding energy. Assuming that the liquid phase virus concentration is small or its affinity for the adsorbent is very low ($bC_g \ll 1$), C_g can be written as

$$C_g \simeq C^*/Q^\circ b. \qquad (32)$$

This assumption is reasonable and does not limit the virus transport model, because liquid phase virus concentrations present in the subsurface are expected to be relatively low. The preceding relationship is essentially a linear isotherm which does not differ from a Freundlich isotherm with unity exponent.

In view of (2), (30), and (32) the following substitutions

$$r_1 = k \qquad r_2 = k/Q^\circ b, \qquad (33)$$

can be employed in the general solutions (28) and (29) to obtain the corresponding S model solutions for constant flux and constant concentration boundary conditions, respectively.

Filtration Model (C Model)

Assuming that the colloid filtration theory is applicable to virus transport, the rate of virus filtration is defined as [*Herzig et al.*, 1970]

$$\frac{\rho}{\theta}\frac{\partial C^*(t,x)}{\partial t} = k_c C(t,x) - k_r \frac{\rho}{\theta} C^*, \qquad (34)$$

where C^* is now the virus concentration retained in the porous medium by the filtration process, and k_c is the clogging rate constant; k_r is the declogging rate constant. The rate of virus filtration depends on the interstitial velocity, suspended virus concentration, and filter coefficient. Although colloid filtration is a time dependent process where deposited colloids may alter the surface structure as well as the porosity of the filtering medium and consequently lead to a variable filter coefficient, for the filtration of submicron particles like viruses it is assumed that no change in the filter coefficient occurs progressively in time. The clogging rate constant can be written as

$$k_c = U\phi F(C^*), \qquad (35)$$

where ϕ is the filter coefficient, and $F(C^*)$ accounts for variations of porosity with increasing particle attachment. When there is no particle-particle interaction ("clean" media), $F(C^*)$ is assumed to be 1.

In view of (2) and (34) the following substitutions

Table 1. Model Parameters for Simulations

Parameter	Value	Reference
b	1.05×10^{-11} mL/virus	*Vilker* [1981]
Q°	1.89×10^8 sites/mg	*Vilker* [1981]
ρ	1.5 g/cm^3	*Yates and Ouyang* [1992]
θ	0.25	*Park et al.* [1992]

$$r_1 = k_c \qquad r_2 = k_r\rho/\theta, \qquad (36)$$

can be employed in the general solutions (28) and (29) to obtain the corresponding C model solutions for constant flux and constant concentration boundary conditions, respectively.

Model Simulations and Discussion

To illustrate the effect of the parameters of the nonequilibrium adsorption model (S model) and filtration model (C model), temporal and spatial virus distributions have been calculated for a variety of situations for both of the boundary conditions considered. For presentation purposes, calculated concentrations were normalized by the source concentration. The integrals in (28) and (29) were evaluated by the extended Simpson's rule [*Press et al.*, 1992]. Unless otherwise specified, breakthrough curves are predicted at a distance $x = 9$ cm downstream from the source, whereas snapshots are given at $t = 10$ days. The fixed parameter values used for the calculations are shown in Table 1, whereas the ranges of attachment and inactivation parameter values used for model simulations are adopted from *Reddy et al.* [1981], *Vilker* [1981], and *Matthess et al.* [1988].

The general solution modified for the S model for the case of constant flux boundary condition is employed to investigate the effect of the mass transfer rate and the two inactivation constants on suspended virus concentration. In Figures 1–3, we

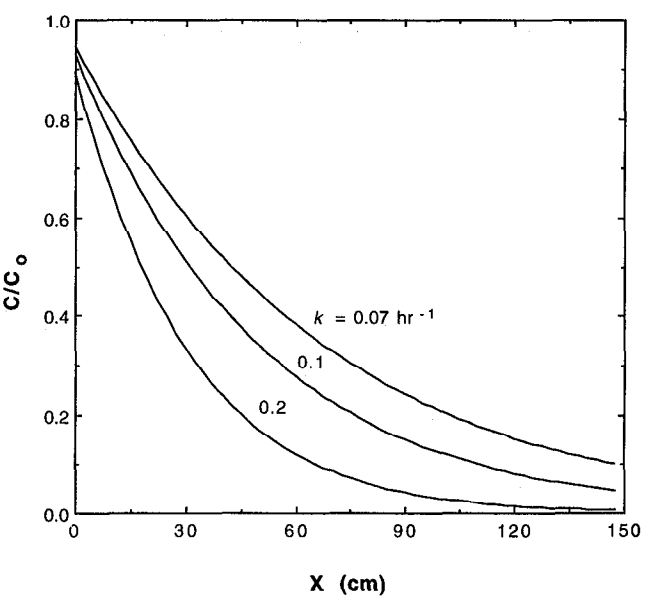

Figure 1. Variation of normalized concentration with distance and mass transfer rate constant as predicted by the S model with constant flux inlet boundary condition ($t = 240$ hours, $D = 15$ cm^2/h, $U = 4$ cm/h, $\lambda = 0.006$ d^{-1}, and $\lambda^* = 0.003$ d^{-1}).

have plotted normalized concentration profiles for three different mass transfer and inactivation rate constants. These illustrations indicate that the liquid phase virus concentration decreases with increasing k, λ, and λ^*. Furthermore, an increase in λ^* leads to a decrease in C_g, and consequently an increase in the rate of virus adsorption onto the solid matrix (see (30)), which causes a reduction in the suspended virus concentration. Here, it is implicitly assumed that C_g is not affected by inactivated viruses still occupying adsorption sites; this assumption is reasonable for low concentrations but can only be verified experimentally. For the case where $\lambda^* = \mathcal{H}$ the parameter $\mathcal{B}$ is zero (see (6)), and the last term of the virus transport model (4) vanishes, which implies that the rate of inactivation of the adsorbed viruses equals the mass transfer–limited rate of adsorption. However, when $\lambda^* > \mathcal{H}$, which implies the inactivation rate of adsorbed viruses is considerable compared to the mass transfer–limited rate of adsorption, the normalized concentration of suspended viruses, instead of increasing and reaching asymptotically the value of 1, reaches a point of maximum concentration and then decreases to a minimum asymptotic value.

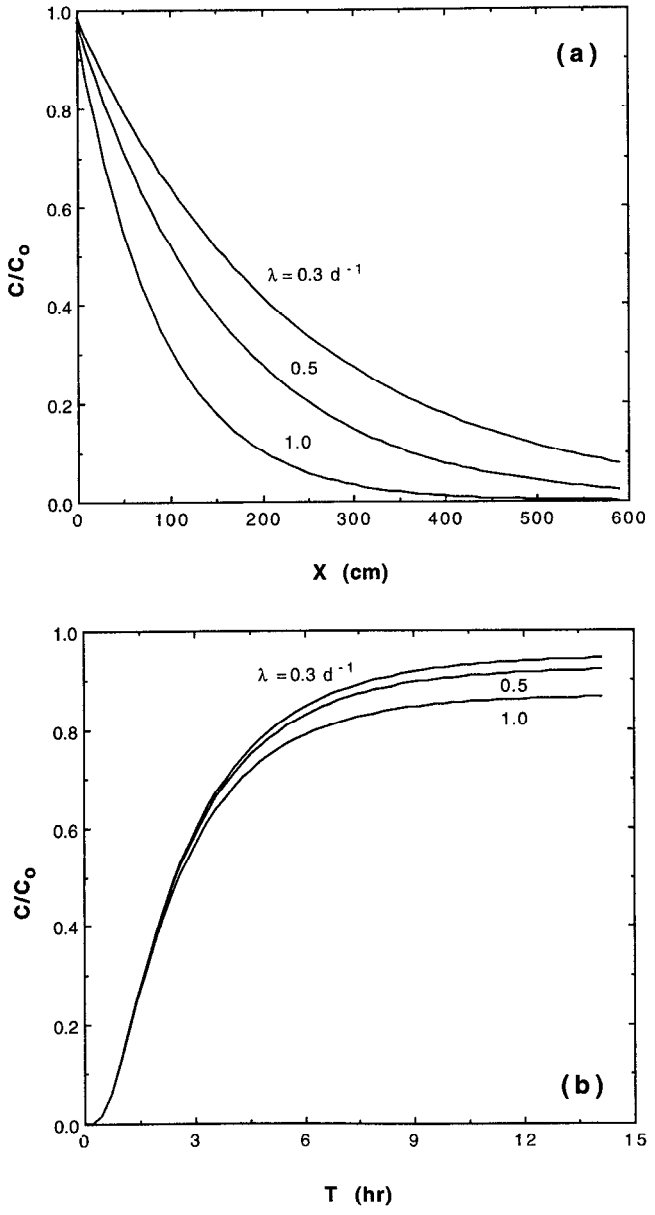

Figure 2. Effect of inactivation constant of suspended viruses on (a) spatial and (b) temporal normalized virus distribution predicted by the S model with constant flux inlet boundary condition (t = 240 hours, x = 9 cm, D = 15 cm^2/h, U = 4 cm/h, λ^* = 0 d^{-1}, and k = 0.005 h^{-1}).

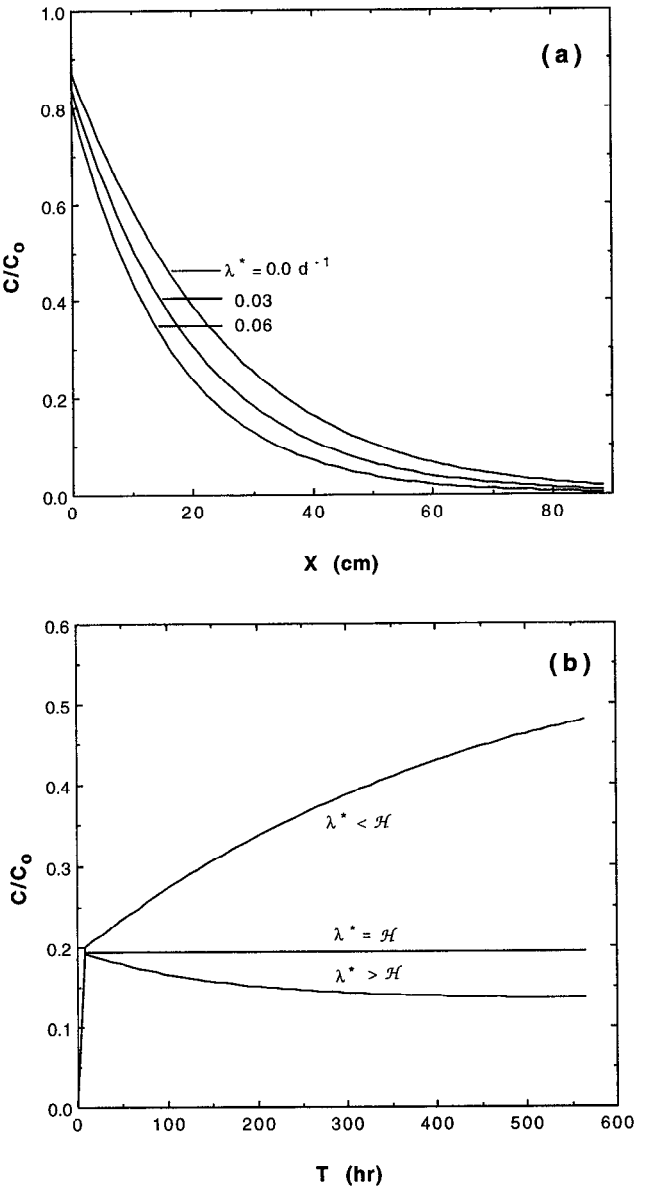

Figure 3. Effect of inactivation constant of adsorbed virus on (a) spatial and (b) temporal normalized virus distribution predicted by the S model with constant flux inlet boundary condition (t = 240 hours, x = 12 cm, D = 15 cm^2/h, U = 4 cm/h, λ = 0.25 d^{-1}, and k = 0.6 h^{-1}).

The general solution modified for the C model with constant flux boundary condition is employed to investigate the effect of the model parameters on liquid phase virus concentration. Normalized concentration profiles for three different clogging and declogging rate constants are presented in Figures 4a and 4b. These snapshots indicate that the suspended virus concentration increases with decreasing k_c and increasing k_r, due to the decreased amount of filtered viruses. The trends of the

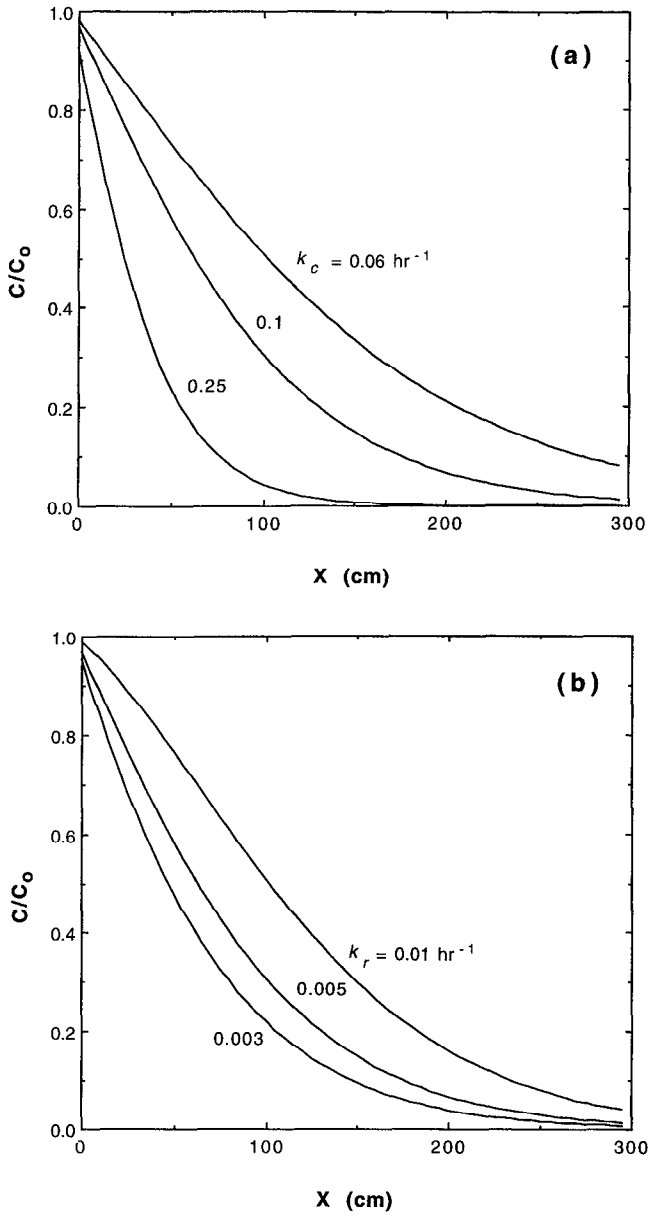

Figure 4. Variation of normalized suspended virus concentration with distance and (a) clogging rate constant and (b) declogging rate constant as predicted by the C model with constant flux inlet boundary condition (t = 240 hours, D = 15 cm^2/h, U = 4 cm/h, λ = 0.006 d^{-1}, and λ^* = 0.003 d^{-1}).

breakthrough and snapshots describing the effects of both inactivation constants are similar to the corresponding trends generated by the S model.

In order to investigate the differences between the two boundary conditions considered in this work, simulated breakthrough curves using (28) and (29) of the S model are plotted in Figure 5 for two different Peclet numbers ($Pe = U\ell/D$, where ℓ is a characteristic or reference length). The differences in the liquid phase virus concentrations due to the different boundary conditions become negligible with increasing Pe. This result is expected, because by decreasing the hydrodynamic dispersion coefficient and increasing the interstitial velocity the boundary conditions (9) and (10) become approximately equivalent.

It has been shown by *van Genuchten and Parker* [1984], *Batu and van Genuchten* [1990], and *Leij et al.* [1991] that improper use of boundary conditions may lead to errors in conservation of mass. Assuming that the total virus mass flux entering through the inlet boundary is constant, we can test whether the inlet boundary condition used satisfies mass conservation in the system for the case where mass loss due to inactivation processes is neglected. Following the work of *van Genuchten and Parker* [1984], the relative virus mass balance error, E, can be defined as

$$E = E_C + E_{C^*} - 1 = \frac{1}{UtC_0}\int_0^\infty C(t, x)\, dx + \frac{\rho}{\theta UtC_0}\int_0^\infty C^*(t, x)\, dx - 1, \quad (37)$$

where the term UtC_0 is the mass of viruses entering the system at the inlet boundary over the time period t, and the integrals on the right-hand side of the preceding equation represent the mass of viruses suspended in solution and deposited onto the solid matrix, respectively, present in the system at time t. In view of (3) the integral expression for the deposited virus concentration in (37) can be written as

$$E_{C^*} = \frac{r_1}{UtC_0}\int_0^\infty \int_0^t C(\tau, x) \exp\left[-\frac{r_2\theta}{\rho}(t - \tau)\right] d\tau\, dx. \quad (38)$$

The multiple integral expressions are evaluated numerically. The total relative mass errors for the two boundary conditions are compared by plotting E as a function of Peclet number (see Figure 6). The comparison indicates that the relative mass

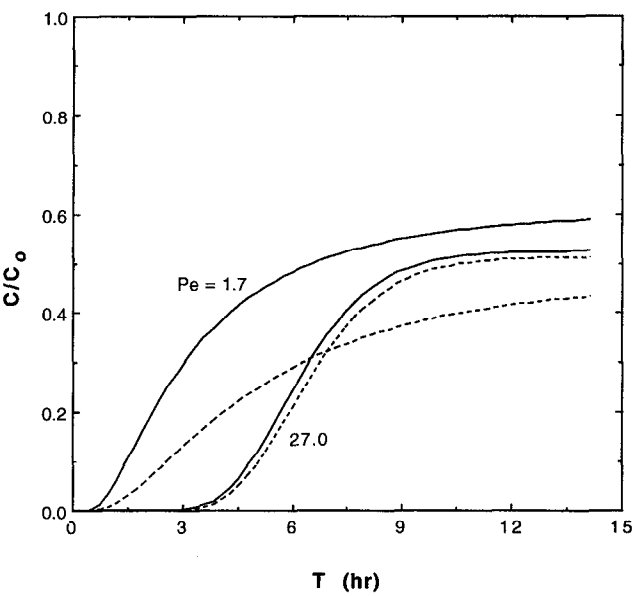

Figure 5. Effect of inlet boundary condition on temporal normalized virus distribution for different Pe values as predicted by the S model (ℓ = 30 cm, $\lambda = \lambda^* = 0$ d^{-1}, and k = 0.1 h^{-1}). Solid and dashed lines represent the constant concentration and the constant flux boundary condition, respectively.

balance error for the constant concentration boundary condition is minimized with increasing Pe. Therefore the discrepancies in the normalized concentrations between the two boundary conditions shown in Figure 5 are attributable to this relative mass balance error caused by the constant concentration boundary condition.

Most of the mathematical models available for transport of microorganisms in porous media employ temperature independent inactivation rate coefficients. However, *Reddy et al.* [1981] and *Yates et al.* [1985] have shown that the inactivation rate is temperature dependent and have presented empirical expressions that relate the inactivation rate to temperature. The equation presented by *Reddy et al.* [1981] represents the relationship between two inactivation rate constants at two different temperatures

$$\lambda_2 = (\lambda_1)1.07^{(T_2-T_1)}, \tag{39}$$

where λ_1 and λ_2 denote the inactivation rate constants at temperatures T_1 and T_2 in degrees Celsius, respectively; while the correlation by *Yates et al.* [1985] determines an average inactivation rate constant at a given temperature

$$\lambda = 0.018T - 0.144, \tag{40}$$

where λ is expressed in $\log_{10}$ (PFU) per day, and PFU is plaque-forming units. Both expressions indicate that the inactivation rate increases with temperature. *Yates and Ouyang* [1992] suggested that the inactivation rate constants of adsorbed (or filtered) viruses are one half of the constants for suspended viruses ($\lambda^* = \lambda/2$). To illustrate the effect of temperature on suspended virus concentration (see Figure 7), we employed correlation (39) and the general analytical solutions modified for S and C models with constant flux boundary condition, for the case of *Poliovirus* ($\lambda = 0.04$ d^{-1} at $T = 4$°C [*Reddy et al.*, 1981]). It is shown in Figure 7 that an increase in temperature leads to an increase in the inactivation rate and, consequently, to a decrease in the suspended virus concentration for both models.

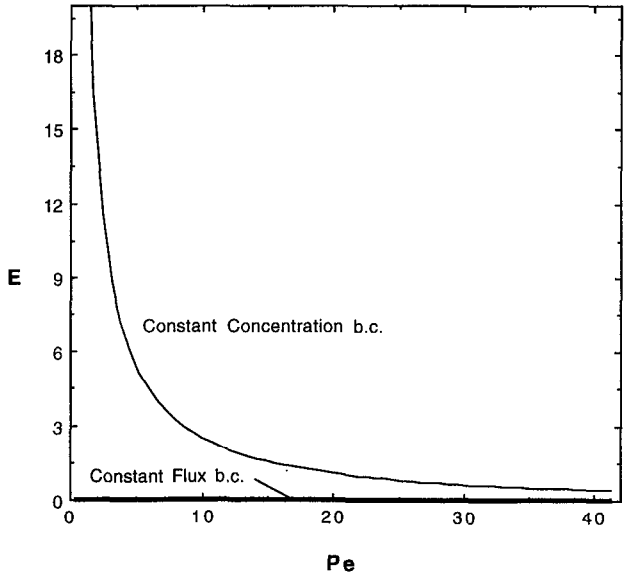

Figure 6. Variation of the relative mass error for constant flux and constant concentration boundary conditions obtained by S model as a function of Pe ($t = 240$ hours, $\ell = 1000$ cm, $\lambda = \lambda^* = 0$ d^{-1}, and $k = 0.01$ hr^{-1}).

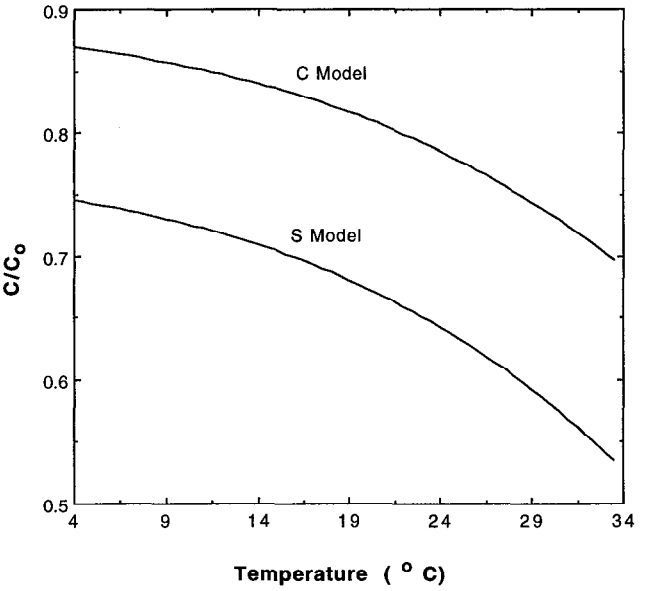

Figure 7. Variation of normalized suspended virus concentration versus groundwater temperature ($t = 240$ hours, $x = 9$ cm, $D = 15$ cm^2/h, $U = 4$ cm/h, $k = 0.1$ hr^{-1}, $k_c = 0.1$ hr^{-1}, and $k_r = 0.005$ hr^{-1}).

The general solution for the case of constant flux boundary condition (equation (28)) was evaluated by simulating the bacteriophage *MS*-2 breakthrough response from the second column experiment published by *Bales et al.* [1991]. The unknown parameters were obtained by a nonlinear least square regression method [*Kahaner et al.*, 1989]. Given that for the particular experimental data set $\theta = 0.35$, $\rho = 1.6$ g/cm^3, and $U = 13.32$ cm/h, the estimated parameters are $D = 31.75$ cm^2/h, $r_1 = 0.79$ h^{-1}, $r_2 = 9.58$ g mL^{-1} h^{-1}, and $\lambda = \lambda^* \simeq 0$. The estimated values of the inactivation rate constants were expected to be approximately zero because the experiment was run at 4°C in order to eliminate viral inactivation [*Bales et al.*, 1991]. For the nonequilibrium adsorption case, in view of (33), $k = 0.79$ h^{-1} and $Q^\circ b = 8.27 \times 10^{-5}$ mL/mg. For the case of virus filtration, in view of (36), $k_c = 0.79$ h^{-1} and $k_r = 2.09$ h^{-1}. The experimental data together with the model simulated profile are shown in Figure 8. Good agreement between the experimental data and the simulated concentration history is shown.

Summary and Conclusions

One-dimensional virus transport in homogeneous porous media was modeled by accounting for first-order rate inactivation for suspended and attached viruses and two different attachment processes: nonequilibrium adsorption (S model) and modified colloid filtration (C model). Since the two physically different attachment processes have identical mathematical forms, only one generalized partial differential equation was solved analytically for both constant flux and constant concentration boundary conditions using Laplace transform techniques. The specific analytical solution for each model can be obtained by substituting the appropriate parameters corresponding to either adsorption or filtration.

The effect of model parameters and boundary conditions on

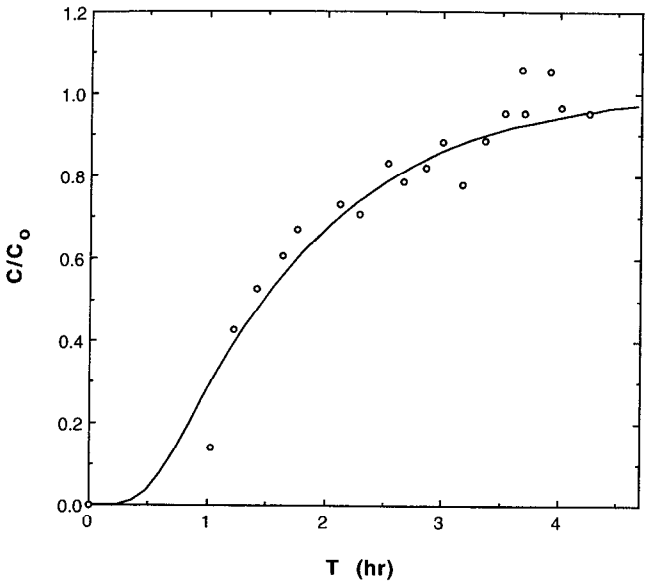

Figure 8. Bacteriophage *MS-2* normalized concentration breakthrough data adopted from *Bales et al.* [1991] (open circles) and simulated concentration history (solid curve).

liquid phase virus concentration was investigated. The virus concentration was found to be mostly sensitive to the mass transfer rate constant for the S model and to the clogging/declogging rate constants for the C model, as well as to the inactivation rate constants. It was demonstrated that the constant flux boundary condition leads to conservation of mass. Furthermore, it was shown that the suspended virus concentration decreases considerably with increasing subsurface temperature.

The results of this investigation are well suited for interpretation and evaluation of transport parameters from laboratory-packed column experiments and possibly some field studies where the assumption of one-dimensional flow under constant hydrodynamic and physicochemical parameters is valid. The methodology of this work can provide a starting point for generalization to the solution of more complicated physical systems and multidimensional virus transport models.

Notation

$\mathcal{A}$ defined in (5), t^{-1}.
b constant related to the bonding energy, L^3/M.
$\mathcal{B}$ defined in (6), t^{-2}.
C concentration of virus in suspension (liquid phase), M/L^3.
C_0 source concentration, M/L^3.
C^* sorbed virus concentration (virus mass/solid mass), M/M.
C_g concentration of virus directly in contact with solids, M/L^3.
D hydrodynamic dispersion coefficient, L^2/t.
E relative mass balance error, defined in (37).
erfc $[x]$ complementary error function, equal to $(2/\pi^{1/2}) \int_x^\infty e^{-z^2}\, dz$.
$\mathcal{H}$ defined in (7), t^{-1}.
$I_0[\ ]$ modified Bessel function of first kind of order zero.
$J_0[\ ]$ Bessel function of first kind of order zero.
k mass transfer rate constant, t^{-1}.
k_c clogging rate constant, t^{-1}.
k_r declogging rate constant, t^{-1}.
k_1 forward reaction rate, t^{-1}.
k_2 reverse reaction rate, t^{-1}.
ℓ characteristic or reference length, L.
$\mathcal{L}^{-1}$ Laplace inverse operator.
M defined in (17a).
N defined in (17b).
Pe Peclet number, equal to $U\ell/D$.
PFU plaque-forming units.
Q° Langmuir monolayer capacity, M/M.
r_1 forward rate coefficient, t^{-1}.
r_2 reverse rate coefficient, M/L^3t.
s Laplace transform variable with respect to time.
t time, t.
T temperature, °C.
U average interstitial velocity, L/t.
x spatial coordinate in the longitudinal direction, L.
z arbitrary argument.
$\alpha_1, \alpha_2, \alpha_3$ constants.
γ Laplace transform variable with respect to space.
ε fractional void volume, L^3/L^3.
ζ dummy integration variable.
θ porosity (liquid volume/porous medium volume), L^3/L^3.
Θ defined in (21).
λ inactivation constant of suspended viruses, t^{-1}.
λ^* inactivation constant of adsorbed (or filtered) viruses, t^{-1}.
ρ bulk density of the solid matrix (solids mass/aquifer volume), M/L^3.
τ dummy integration variable.
ϕ filter coefficient, L^{-1}.

Subscripts

cc constant concentration boundary condition.
cf constant flux boundary condition.

Acknowledgments. The authors acknowledge Stanley Grant and Terese Olson for many stimulating discussions. This work was sponsored by the National Water Research Institute, under award NWRI/EPA 92-04. However, the manuscript has not been subjected to the agency's peer and administrative review and therefore does not necessarily reflect the views of the agency, and no official endorsement should be inferred. Correspondence regarding this paper should be addressed to C.V.C.

References

Abramowitz, M., and I. A. Stegun, *Handbook of Mathematical Functions*, 1046 pp., Dover, Mineola, N. Y., 1972.

Bales, R. C., S. R. Hinkle, T. W. Kroeger, and K. Stocking, Bacteriophage adsorption during transport through porous media: Chemical perturbations and reversibility, *Environ. Sci. Technol.*, *25*(12), 2088–2095, 1991.

Batu, V., and M. T. van Genuchten, First- and third-type boundary conditions in two-dimensional solute transport modeling, *Water Resour. Res.*, *26*(2), 339–350, 1990.

Chrysikopoulos, C. V., P. V. Roberts, and P. K. Kitanidis, One-dimensional solute transport in porous media with partial well-to-well recirculation: Application to field experiments, *Water Resour. Res.*, *26*(6), 1189–1195, 1990.

Corapcioglu, M. Y., and A. Haridas, Transport and fate of microorganisms in porous media: A theoretical investigation, *J. Hydrol., 72*, 149–169, 1984.

Gerba, C. P., Applied and theoretical aspects of virus adsorption to surfaces, *Adv. Appl. Microb., 30*, 133–168, 1984.

Grant, S. B., E. J. List, and M. E. Lidstrom, Kinetic analysis of virus adsorption and inactivation in batch experiments, *Water Resour. Res., 29*(7), 2067–2085, 1993.

Grosser, P. W., A one-dimensional mathematical model of virus transport, paper presented at the Second International Conference on Ground-Water Quality Research, Univ. Cent. for Water Res., Okla. State Univ., Tulsa, Okla., March 26–29, 1984.

Harvey, R. W., and S. P. Garabedian, Use of colloid filtration theory in modeling movement of bacteria through a contaminated sandy aquifer, *Environ. Sci. Technol., 25*(1), 178–185, 1991.

Herzig, J. P., D. M. Leclerc, and P. LeGoff, Flow of suspensions through porous media—Application to deep filtration, *Ind. Eng. Chem., 62*(5), 8–35, 1970.

Hurst, C. J., C. P. Gerba, and I. Cech, Effects of environmental variables and soil characteristics on virus survival in soil, *Appl. Environ. Microb., 40*, 1067–1079, 1980.

Kahaner, D., C. Moler, and S. Nash, *Numerical Methods and Software*, Prentice-Hall, Englewood Cliffs, N. J., 1989.

Lapidus, L., and N. R. Amundson, Mathematics of adsorption in beds, VI, The effect of longitudinal diffusion in ion exchange and chromatographic columns, *J. Phys. Chem., 56*, 984–988, 1952.

Leij, F. J., T. H. Skaggs, and M. T. van Genuchten, Analytical solutions for solute transport in three-dimensional semi-infinite porous media, *Water Resour. Res., 27*(10), 2719–2733, 1991.

Matthess, G., A. Pekdeger, and J. Schroeter, Persistence and transport of bacteria and viruses in groundwater: A conceptual evaluation, *J. Contam. Hydrol., 2*, 171–188, 1988.

Morel, F., *Principles of Aquatic Chemistry*, John Wiley, New York, 1983.

Park, N., T. N. Blanford, and P. S. Huyakorn, VIRALT: A modular semi-analytical and numerical model for simulating viral transport in ground water, report, Int. Ground Water Model. Cent., Colo. Sch. of Mines, Golden, 1992.

Press, W. H., S. A. Teukolsky, W. T. Vetterling, and B. P. Flannery, *Numerical Recipies*, 963 pp., Cambridge University Press, New York, 1992.

Reddy, K. R., R. Khaleel, and M. R. Overcash, Behavior and transport of microbial pathogens and indicator organisms in soils treated with organic wastes, *J. Environ. Qual., 10*(3), 255–266, 1981.

Roberts, G. E., and H. Kaufman, *Table of Laplace Transforms*, 367 pp., W. B. Saunders, Philadelphia, Pa., 1966.

Sobsey, M., Transport and fate of viruses in soil, in Microbial Health Considerations of Soil Disposal of Domestic Wastewaters, *Publ. EPA-600/9-83-017*, pp. 174–213, Environ. Prot. Agency, Washington, D. C., 1983.

Teutsch, G., K. Herbold-Paschke, D. Tougianidou, T. Hahn, and K. Botzenhart, Transport of microorganisms in the underground—Processes, experiments, and simulation models, *Water Sci. Technol., 24*(2), 309–314, 1991.

Tim, U. S., and S. Mostaghimi, Model for predicting virus movement through soils, *Ground Water, 29*(2), 251–259, 1991.

van Genuchten, M. T., and J. C. Parker, Boundary conditions for displacement experiments through short laboratory soil columns, *Soil Sci. Soc. Am. J., 48*, 703–708, 1984.

Vilker, V. L., Simulating virus movement in soils, in *Modeling Waste Renovation: Land Treatment*, edited by I. K. Iskandar, pp. 223–253, John Wiley, New York, 1981.

Vilker, V. L., L. H. Frommhagen, R. Kamda, and S. Sundaram, Application of ion exchange/adsorption models to virus transport in percolating beds, *AIChE Symp. Ser., 74*(178), 84–92, 1978.

Yates, M. V., and Y. Ouyang, VIRTUS, a model of virus transport in unsaturated soils, *Appl. Environ. Microb., 58*(5), 1609–1616, 1992.

Yates, M. V., and S. R. Yates, Modeling microbial fate in the subsurface environment, *Crit. Rev. Environ. Control, 17*(4), 307–344, 1988.

Yates, M. V., C. P. Gerba, and L. M. Kelly, Virus persistence in groundwater, *Appl. Environ. Microb., 49*, 778–781, 1985.

C. V. Chrysikopoulos and Y. Sim, Department of Civil and Environmental Engineering, University of California, Irvine, CA 92717. (e-mail: costas@max.eng.uci.edu)

(Received May 27, 1994; revised January 10, 1995;
accepted January 12, 1995.)

Correction to "Analytical models for one-dimensional virus transport in saturated porous media" by Youn Sim and Constantinos V. Chrysikopoulos

In the paper "Analytical models for one-dimensional virus transport in saturated porous media" by Youn Sim and Constantinos V. Chrysikopoulos (*Water Resources Research*, *31*(5), 1429–1437, 1995), the expression (2) for the rate of virus attachment onto the solid matrix is incorrect. The error is associated only with the description of parameter r_2 and does not affect the derived analytical solutions. It should be noted, however, that only simulations for $\lambda^* > 0$ (Figures 1, 3, and 4) are influenced by this correction. Reevaluation of the results follows.

The parameter r_2 following (2) on page 1430 should be defined as "effective" reverse rate coefficient to also account for inactivation of adsorbed (or filtered) viruses. For the Nonequilibrium Adsorption Model (S Model) equation (30) should be replaced by the following:

$$\frac{\rho}{\theta}\frac{\partial C^*(t, x)}{\partial t} = k[C(t, x) - C_g(t, x)] - \frac{\rho}{\theta}\lambda^* C^*(t, x). \qquad (30)$$

As a consequence,

$$r_2 = \frac{k}{Q^\circ b} + \frac{\rho}{\theta}\lambda^*. \qquad (33b)$$

Similarly, for the Filtration Model (C Model) equation (34) should be replaced by the following:

$$\frac{\rho}{\theta}\frac{\partial C^*(t, x)}{\partial t} = k_c C(t, x) - \frac{\rho}{\theta}(k_r + \lambda^*)C^*(t, x). \qquad (34)$$

As a consequence,

$$r_2 = \frac{\rho}{\theta}(k_r + \lambda^*). \qquad (36b)$$

Reevaluation of the normalized virus concentration curves in Figures 1, 3a, and 4 leads to similar results. However, in Figure 3b, the case of $\lambda^* > \mathcal{H}$ is no longer an option. The reason is that in view of the corrected r_2, the parameter $\mathcal{H} = \theta r_2/\rho$ can never be less than λ^*.

The solutions derived in this work, unlike other analytical solutions present in the literature, account for first-order inactivation of suspended and adsorbed viruses with different inactivation constants ($\lambda \neq \lambda^*$). This assumption is consistent with the work of *Hurst et al*. [1980], *Gerba* [1984] and *Yates and Yates* [1988]. For each of the two models considered, analytical solutions were derived for both constant flux and constant concentration upstream boundary conditions. In view of the redefined "effective" reverse rate coefficient (36b), the solution to the C Model for the constant concentration boundary condition was tested against a solution to a bacterial transport model presented by *Corapcioglu and Haridas* [1985], which accounts for microbial decay of suspended and attached bacteria with identical rates ($\lambda = \lambda^*$). For this limiting case the two solutions result in almost identical concentration profiles.

References

Corapcioglu, M. Y., and A. Haridas, Microbial transport in soils and groundwater: A numerical model, *Adv. Water Resour*., *8*, 188–200, 1985.

Gerba, C. P., Applied and theoretical aspects of virus adsorption to surfaces, *Adv. Appl. Microb*., *30*, 133–168, 1984.

Hurst, C. J., C. P. Gerba, and I. Cech, Effects of environmental variables and soil characteristics on virus survival in soil, *Appl. Environ. Microb*., *40*, 1067–1079, 1980.

Yates, M. V., and S. R. Yates, Modeling microbial fate in the subsurface environment, *Crit. Rev. Environ. Control*, *17*(4), 307–344, 1988.

(Received December 4, 1995.)

Paper number 96WR00675.
0043-1397/96/96WR-00675$09.00